



CCUS: 4014878

Multi-Resolution Simulation for Efficient Pressure & Stress Calculation in Large-Scale CO₂ Storage Using Pseudosteady State Pressure as Spatial Coordinate

Kazuyuki Terada*, Akhil Datta-Gupta, Michael J. King. Texas A&M University.

Copyright 2024, Carbon Capture, Utilization, and Storage conference (CCUS) DOI 10.15530/ccus-2024-4014878

This paper was prepared for presentation at the Carbon Capture, Utilization, and Storage conference held in Houston, TX, 11-13 March.

The CCUS Technical Program Committee accepted this presentation on the basis of information contained in an abstract submitted by the author(s). The contents of this paper have not been reviewed by CCUS and CCUS does not warrant the accuracy, reliability, or timeliness of any information herein. All information is the responsibility of, and, is subject to corrections by the author(s). Any person or entity that relies on any information obtained from this paper does so at their own risk. The information herein does not necessarily reflect any position of CCUS. Any reproduction, distribution, or storage of any part of this paper by anyone other than the author without the written consent of CCUS is prohibited.

Abstract

Large-scale CO₂ injection operation causes pressure and stress changes in subsurface with potential geomechanical risks such as ground surface uplift, caprock failure and CO₂ leakage through fractures, or/and reactivation of faults and triggering induced seismicity. Although existing dynamic reservoir and geomechanics simulation tools can assess these operational risks, the excessive computational time remains a major bottleneck for large-scale CCS applications. We propose a rapid coupled flow and geomechanics simulation approach that uses pseudosteady state pressure as spatial coordinate (PSS-SIM), focusing on efficient pressure and mean stress change calculation caused by CO₂ injection. PSS-SIM can speed up the coupled simulation by more than an order-of-magnitude while accounting for model heterogeneity, and allows us for quick evaluation of geomechanical risks of CO₂ injection operation under geologic uncertainty. The proposed simulation workflow accelerates pressure and mean stress change calculation in CO₂ injection simulation by multi-resolution grid coarsening based on PSS pressure contours. PSS-SIM can be seen as generalization of the Fast Marching Method (FMM) based multi-resolution coupled flow and geomechanics simulation for unconventional reservoirs (Terada et al., 2023) to CCS applications that replaces Diffusive Time-Of-Flight (DTOF) with PSS pressure solution as the choice of spatial coordinate because of the expected flow patterns in CCS reservoirs. PSS-SIM utilizes one-way coupling scheme to facilitate field-scale applications, and is capable of computing pressure and mean stress change with more than an order-of-magnitude less computational time compared to fine-scale simulation. The validity of pressure change calculation along PSS pressure contours in high permeability reservoirs is validated with a synthetic 3-D fine-scale simulation. The applicability to field-scale problems is demonstrated with simulation of a large-scale CO₂ storage test in saline aquifer for rapid geomechanical risk assessment. Snapshots of simulated pressure change from PSS-SIM showed consistent results with fine-scale simulation with capability to calculate mean stress as additional outputs.

The proposed multi-resolution simulation workflow is a novel approach to significantly reduce computational time of CO₂ injection simulation that allows us for quick assessment of geomechanical risks in CCS operation associated with pressure and stress changes.

Introduction

Carbon dioxide (CO₂) storage is a part of the Carbon Capture Utilization and Storage (CCUS) process, where significant amount of CO₂ is usually injected into depleted reservoirs or deep saline aquifers and can be stored in the pore spaces over a geologic timescale due to the combination of physical and geochemical trapping mechanisms. In the early stages of the storage process, the principal means to store CO₂ in geological formations is to trap CO₂ below low permeability seals (caprocks) (IPCC, 2005). While the maximum bottom-hole pressure at the injection well is usually the major limiting factor for the operational efficiency, the pressure increase caused by continuous industrial-scale CO₂ injection may be another constraint due to geomechanical risks linked to the pressure buildup. Pore pressure and the associated rock deformation/stress changes have a potential to reactivate existing faults and fractures, which can cause surface uplift, leakage of CO₂, and induced seismicity that may concern local community.

Dynamic reservoir simulation is costly yet one of the most reliable tools for evaluating storage efficiency and the operational risks that is capable of accounting for reservoir heterogeneity and complex physics involved in CO₂ injection. Injectivity/storage capacity as metrics for effectiveness of the storage operation primarily depends on reservoir heterogeneity and connected pore volume to injection wells, but proper characterization of the overlying/underlying seals is also important due to its effects on pressure buildup in/around the reservoir (Zhou et al., 2008). Pruess and Garcia (2002) is one of the studies which applied multi-phase flow simulation for modeling of CO₂ injection into saline aquifers accounting for the loss of CO₂ from storage through discharge along a fault zone. The use of coupled flow and geomechanics simulation has also become more popular in CCS studies with increasing attentions to the geomechanical risks. Winterfeld and Wu (2017) presented a thermal-hydrological-mechanical (THM) reservoir simulator that can assess the sealing capability of caprocks, and in Zheng et al. (2020), coupled simulation was integrated in their optimization framework to maximize CO₂ storage while minimizing geomechanical risks under geologic uncertainty.

Despite its advantages, using reservoir simulation for field-scale CCS problems remains computationally challenging as typical CO₂ storage models are required to cover large geologic domain including caprocks, basement and reservoir. The computational time of more complex models such as compositional simulation and coupled flow, thermal & geomechanics simulation can be easily prohibitive for the large models, especially when hundreds of simulation runs are required under the geologic uncertainty. Given the demands for quick storage assessment and optimization tools for CCS, there has been significant advances in the areas of Deep Learning (DL)-based workflows that can potentially replace the expensive numerical simulation. To list only a few, Nagao et al. (2023) developed a versatile DL-based workflow for efficient CO₂ plume visualization, uncertainty quantification for predicted CO₂ plume images, and efficient optimization of measurement location and measurement type, and Chen et al. (2022) presented a DL-accelerated history matching workflow for large-scale geologic CO₂ sequestration. One of the typical downsides of the complex DL models is its expensive training time, especially when the workflow utilizes numerical simulation output for its training data since it may require thousands of simulation runs to begin with. On the other hand, any overly simplistic machine learning/analytical models may suffer from the loss of accuracy. Therefore, reliable and fast numerical simulation tools that can balance between accuracy and efficiency are still in great demand for strategic development and optimization of CO₂ storage to enhance the processes such as site screening, well location selection, and risk assessments.

Outside the CCS studies, Fast Marching Method (FMM)-Based Simulation is one of the efficient reservoir simulation techniques with many successful unconventional reservoir applications (Zhang et al., 2016; Fujita et al., 2016; Iino et al., 2017), which accelerates field-scale simulation by more than an order-of-magnitude while accounting for reservoir heterogeneity. FMM-based simulation achieves the significant speed up by transforming the original 3-D problem into a 1-D problem along Diffusive Time-of-Flight (DTOF) coordinate. DTOF is a travel time of pressure front from the well whose contour lines resemble pressure change profile during the production from tight reservoirs, where prolonged transient period is observed. In the recent studies of FMM-based simulation (Chen et al., 2022, Terada et al., 2023), the efficient 1-D simulation technique has been extended to multi-resolution grids scheme and coupled flow and geomechanics. The multi-resolution grids refers to the mixture of high-resolution grids retained around the wells and base 1-D grids, and it is shown to provide balanced accuracy and efficiency to the simulation. Coupling with geomechanics adds the ability to solve a reduced geomechanical variable, mean stress change, efficiently in the same hybrid grids, and also allows more detailed stress-tensor component calculation with additional computational cost.

In this study, we present multi-resolution coupled flow and geomechanics simulation that uses PSS pressure as spatial coordinate (PSS-SIM), as an efficient numerical simulation tool for CO₂ injection modeling. The use of PSS pressure as an alternative spatial coordinate to DTOF was introduced by Kenta and King (2021) for applications in high permeability reservoirs, which may be the case beyond the “prolonged transient” assumptions of FMM-based simulation. In typical high permeability CCS reservoirs surrounded by low permeability seals, pressure is expected to approach PSS at relatively early time of injection. This is the first study to incorporate PSS pressure-based grids with the multi-resolution approach and coupled flow and geomechanics as an extension of the FMM-based simulation to CCS applications. PSS-SIM is primarily designed for rapid prediction of pressure build up in/around the reservoir due to CO₂ injection, but also has the capability to compute the associated mean stress change as additional output at minimal increase of computational cost through coupling with mean-stress based geomechanics (Winterfeld et al., 2015). PSS-SIM is validated using a simple gas injection case with fine-scale simulation for well responses and spatial pressure change solution. PSS-SIM is applied to a large-scale CO₂ storage test involving compositional flow simulation for the multi-million cell model, and the efficient simulation workflow is demonstrated in the context of quick induced seismicity (fault slip) risk assessment following Changqing et al. (2023). This work has been conducted as a part of the Science-informed Machine Learning (ML) for Accelerating Real-Time Decisions in Subsurface Applications (SMART) Initiative which is funded by the US Department of Energy Carbon Storage program for development of reduced-order numerical simulation tool.

Methodology

Spatial Discretization Using Pressure Solution Contours: DTOF vs PSS Pressure

Efficiency of our simulation workflow derives from grid coarsening along pressure solution contours, where the idea originated in FMM-based simulation (Zhang, 2016) that uses DTOF for the spatial discretization. The DTOF is an arrival time of pressure front propagating from a well that is governed by the Eikonal equation (Eq. 1) derived from the high-frequency asymptotic solution of the diffusivity equation (Onishi et al., 2019), and its contours approximate the contours of pressure changes during the transient period. The discretized form of the Eikonal equation (Eq. 2) (Chen et al., 2021) can be efficiently solved for DTOF at each cell by using Fast Marching Method (FMM) (Sethian, 1999) based on initial reservoir properties prior to simulation, which only takes 0.5~3 seconds per million cells.

$$|\nabla \tau(x)| = \frac{1}{\sqrt{\alpha(x)}}, \alpha(x) = \frac{\lambda_t(x)k(x)}{\phi(x)c_t(x)}, \quad (1)$$

$$\sum_{i=1}^{n_{\text{upstream}}} (\tau_c - \tau_{u,i})^2 T_{A,i} = V_p \mu c_t \quad (2)$$

Here, DTOF is denoted as τ in **Eq. 1** and **Eq. 2**, and subscripts c and u represent the cell of interest and its upstream connections, respectively. Grouping of fine-scale cells along DTOF contours and upscaling of reservoir properties enable transformation of the original 3-D model into a 1-D model along DTOF coordinate. The computational time required for the model transformation process is usually much less than the time for the fine-scale simulation, and the efficient 1-D simulation on the DTOF grids tend to result in more than an order-of-magnitude faster computation than fine-scale simulation while accounting for reservoir heterogeneity reflected on DTOF (**Fig. 1**).

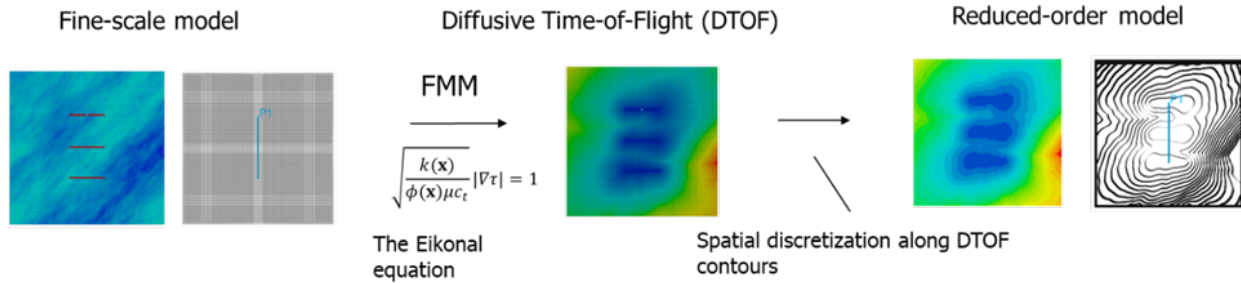


Figure 1. Spatial discretization using transient pressure solution (DTOF) for model order reduction

While DTOF resembles pressure evolution under most circumstances in unconventional reservoirs where transient period elongates, Nakajima and King (2021) proposed PSS pressure as another pressure solution as a choice of spatial coordinate for high permeability reservoirs. One way to obtain PSS pressure solution is to solve **Eq. 3** using 3-D finite difference method, which is essentially to solve simplified reservoir simulation for one time step based on initial reservoir properties assuming dp/dt is uniform. The PSS pressure calculation may take a few seconds to minutes depending on the reservoir complexity, and is a relatively costly calculation than FMM for DTOF. However, the PSS pressure only needs to be calculated once prior to simulation and this pre-processing time can be justified if simulation time is long enough.

$$\frac{1}{\mu} \sum T_{nm} (p_n - p_m) + \frac{1}{\mu} WI (p_n - p_{wf}) = \frac{q_{wf}}{V_{p,connected}} \cdot V_{p,n} \quad (3)$$

Eq. 3 represents the discretized equation for a completion cell, and q_{wf} , $V_{p,connected}$, $V_{p,n}$ denote total fluid extraction from the reservoir, connected pore volume to the well and cell pore volume, respectively. **Fig. 2** compares DTOF and PSS pressure contours for a simple 3-D case, both of which fully account for reservoir heterogeneity. Grid coarsening along different contour shapes of DTOF and PSS pressure will result in two individual 1-D grids that vary in pore volume and transmissibility at each 1-D cell. Main difference between the two pressure solutions is inner/outer boundary conditions and the deviation between two solution contours are more prominent around the corners of the reservoir in **Fig. 2**. Without explicitly accounting for reflection of waves at boundaries, DTOF contours do not reflect boundary effects. Since DTOF represents a travel time of the pressure disturbance from the well, well constraints are not accounted either. The appropriate choice of the pressure solution for the spatial coordinate requires the understandings of reservoir characteristics and expected flow patterns. For typical CO₂ storage simulation, we assume years of CO₂ injection into high permeability zones surrounded by low permeability/impervious seals. Under that circumstances, it is reasonable to expect the initiation of boundary dominated flow at relatively early time of the simulation, and hence we choose PSS pressure for the spatial coordinate in this study. It should be noted that we take advantage of efficiently calculated

DTOF for faster and robust PSS pressure calculation by identifying the connected pore volume to the well through DTOF, which appears in the source term of Eq. 3.

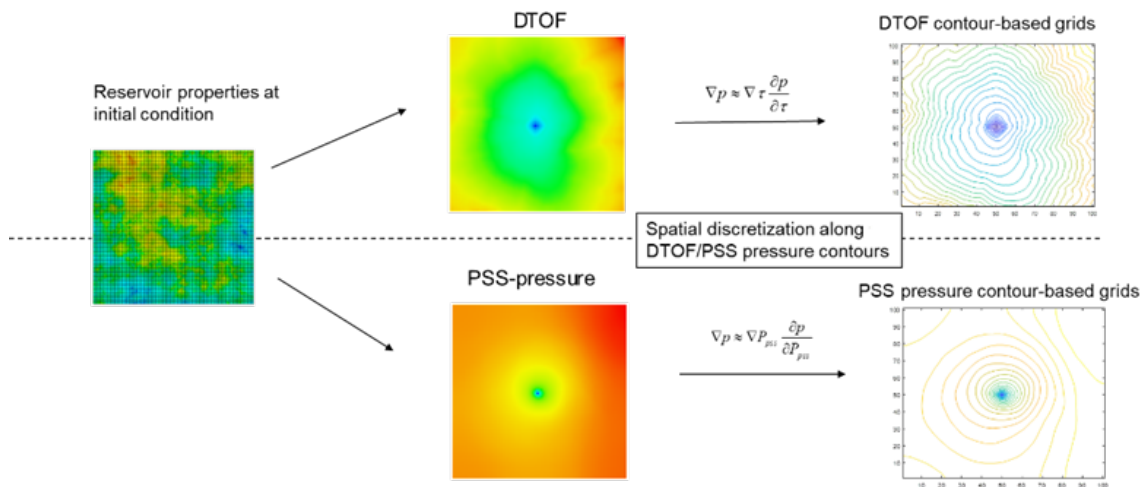


Figure 2. DTOF vs PSS pressure contours

Multi-Resolution Grids Based on PSS Pressure Solution

Multi-resolution grids in FMM-based simulation refers to the combination of fine-scale grids retained around the well (preserved domain) and coarse 1-D grids formed outside the preserved domain as the result of spatial discretization along DTOF, which has been developed to balance between accuracy and efficiency (Chen et al., 2022, Terada et al., 2023). We follow this approach and similarly define preserved domain and 1-D grids region for the PSS pressure-based grids (Fig. 3).

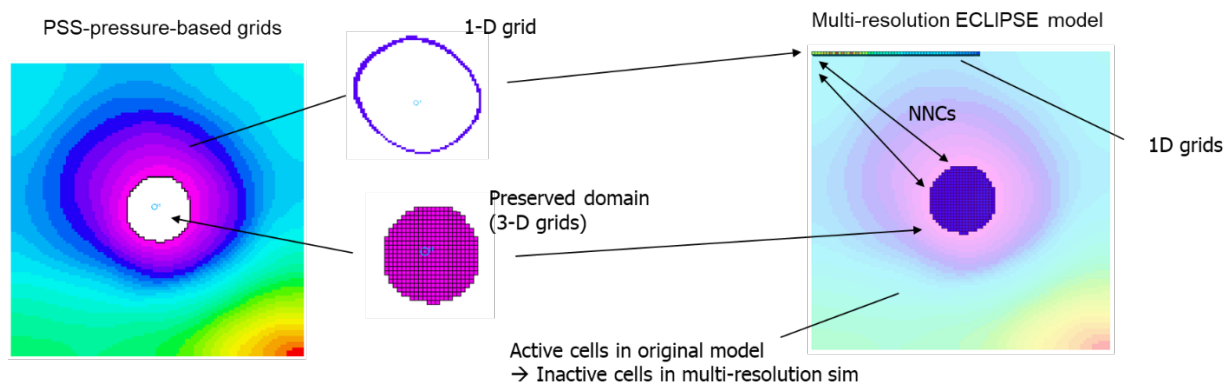


Figure 3. Multi-resolution grids in PSS pressure coordinate

Preserved domain is defined inside a certain PSS pressure contour line specified as a cutoff, and currently the cutoff value is user input to allow for tuning of grid resolution in the context of the accuracy-efficiency trade-off. By design, injection wells are always inside the preserved domain regardless of the cutoff value, and original well index of the fine-scale model is used. The outermost cells of the preserved domain are all connected to the 1st 1-D cell outside the preserved domain through Non Neighbor Connections (NNCs), and subsequent coarse cells have 1-D connections. Based on the original fine-scale model, multi-resolution model can be designed as follows. Fine-scale cells that configure the preserved domain remain active cells and keep their original cell indices in the multi-resolution model, and all other fine-scale cells which are grouped into 1-D cells are converted to inactive cells. This will produce unused

cell locations where the generated 1-D grids and computed cell properties can be assigned to without changing original grid dimension. As a result, the multi-resolution model becomes a 3-D model with many inactive cells and NNCs.

Transmissibility Upscaling

Transmissibility upscaling for PSS pressure-based grids is a part of pre-processing required for flow simulation in the multi-resolution grids. We choose simple flow-based transmissibility upscaling by taking advantage of PSS pressure calculated at every cell for grid coarsening prior to the transmissibility upscaling. **Fig. 4** describes the transmissibility upscaling for a connection between two 1-D grids in the simple schematic. Considering flux conservation at the interface between the two 1-D grids, upscaled transmissibility across the two 1-D cells can be expressed by pressure drops at the interface and across the two 1-D cells, and summation of fine-scale transmissibility at the interface (**Eq. 4**).

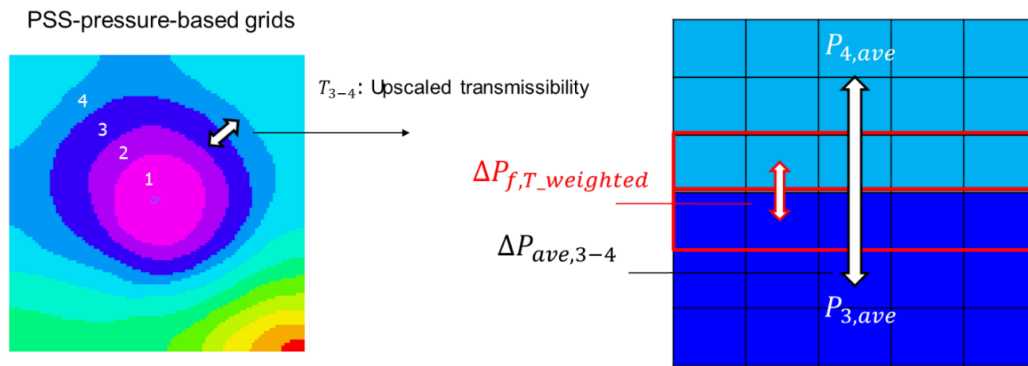


Figure 4. Transmissibility upscaling

$$T_{upscaled} = \sum_{i_face} T_f \cdot \frac{\Delta P_{f,T_weighted}}{\Delta P_{ave}} \quad (4)$$

Here, reference pressure drop at the interface is computed by transmissibility weighted average of corresponding cells, and the pressure drop across the two 1-D cells are computed based on pore-volume weighted average of the coarse-scale grids. For connections between fine-scale grids of preserved domain and the coarsened grid, the transmissibility computed by **Eq. 4** can be distributed for each cell based on its fine-scale transmissibility.

Coupling with Geomechanics in PSS-Pressure Coordinate

Following Terada et al. (2019, 2023), we incorporate Mean Stress (MS)-based geomechanics formulation (**Eq. 5**) proposed by Hu et al. (2013) as the governing equation of the efficient geomechanics module. Although the MS-based formulation is not the most popular form of geomechanics equation, it has been adopted in multiple studies and employed in simulators such as 6X reservoir simulator from Ridgeway Kite and TOUGH2- series (EGS, CSM etc.). Since the MS equation is linear with respect to pressure and mean stress when time-invariant Poisson's ratio and boundary condition are assumed, it can be directly solved for mean stress change from the initial condition that would be caused by pressure increase as a result of CO₂ injection, and takes the following form:

$$\nabla \cdot \left[\frac{3(1-\nu)}{1+\nu} \nabla(\Delta\sigma_m) + b \frac{2(1-2\nu)}{1+\nu} \nabla(\Delta p) \right] = 0, \quad (5)$$

where $\Delta\sigma_m = \sigma_m - \sigma_{m,0}$, $\Delta p = p - p_0$ and $\Delta\sigma_m = 0$ or $\partial(\Delta\sigma_m)/\partial\bar{n} = 0$ at boundaries. Here, temperature and body force are neglected. The MS-based geomechanics formulation (Eq. 5) is adopted in PSS-SIM due to the pressure-like behavior of mean stress change as shown in Terada et al. (2019, 2023), such that flow and geomechanics can be both solved efficiently in the common PSS pressure grids. While MS-based formulation itself is a more efficient form of the geomechanics equation that is solved for a reduced primary variable compared to displacement-based formulation, solving the MS-based equation in multi-resolution grids amplifies the computational benefits. Note that the MS-based geomechanics modeling allows calculation of stress-tensor components as secondary variables through Eq. 6 as shown in Winterfeld et al. (2015).

$$\frac{1}{2}\nabla^2\sigma_x = -b\frac{\partial^2 p}{\partial x^2} - \frac{3}{2(1+\nu)}\frac{\partial^2}{\partial x^2}(\sigma_m + bp) + \frac{3\nu}{2(1+\nu)}\nabla^2(\sigma_m + bp) \tag{6}$$

Eq. 6 is for computation of normal stress in x-direction given pressure and mean stress computed as primary variables. Normal stress components in other directions and shear stresses can be computed similarly for each component independently, hence this calculation is less computationally demanding compared to solving the three components of displacement vector simultaneously as in typical geomechanics model. Since this requires calculation on original fine-scale grids, it is incorporated in our simulation workflow as optional post-processing calculation that comes with additional computation cost. It is worth mentioning that recently semi-analytical solution was presented for the MS-formulation in Wang and Wu (2022). However, the solution requires homogeneous mechanical properties and numerical solution is still required for heterogeneous model.

Simulation Workflow

Fig. 5 summarizes the simulation workflow of PSS-SIM. The workflow is built around the choice of flow simulator to speed up its fine-scale simulation by upgridding/upscaling of the model based on PSS pressure solution. The generated multi-resolution grid is also used for geomechanics simulation. In this study, we use ECLIPSE from SLB as our flow simulator, and it is coupled with an in-house MS-based geomechanics simulator by one-way coupling to facilitate field-scale applications, hence the effects of geomechanics on flow are neglected.

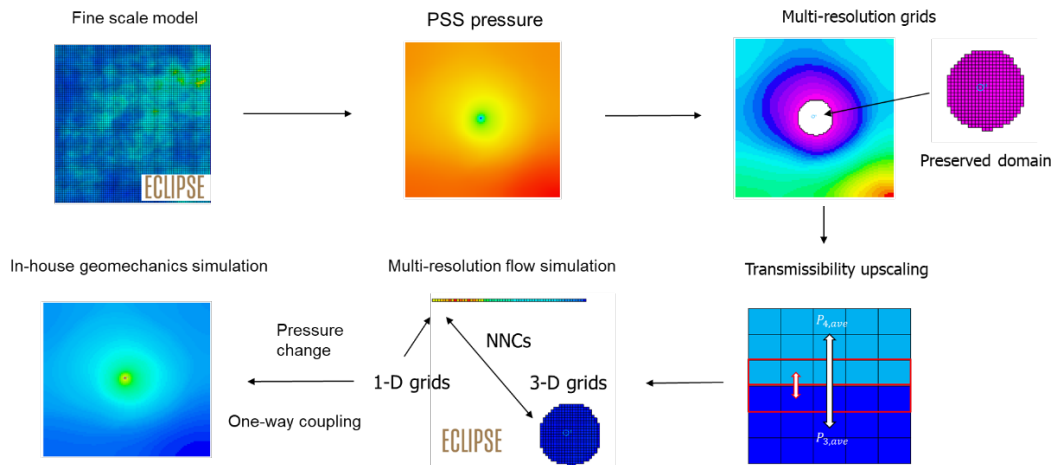


Figure 5. PSS-SIM workflow

The pre-processing begins with calculation of PSS pressure solution based on initial reservoir properties of the fine-scale model. As mentioned in the previous section, DTOF is also quickly computed prior to the PSS pressure calculation using FMM to identify the connected pore volume to the injector that is

required for faster and robust PSS pressure calculation. Next, the reservoir is coarsened along PSS-pressure contours to form 1-D grids and the geometry of the preserved domain is determined based on the user specified cutoff value. Once the upgridding is finished, cell properties and transmissibility for the 1-D grids are upscaled from the fine-scale model to complete the multi-resolution model. In the one-way coupling, flow simulation is run first and feeds pressure change solution to the mean stress geomechanics simulation. Pressure and mean stress changes efficiently solved on the multi-resolution grids can be mapped back to original fine-scale grids for visualization or optional stress-tensor components calculation, which requires 3-D finite difference calculation on the fine-scale grids.

Validation: Pressure Change Calculation on PSS Pressure-Based Grids in Conventional Reservoirs

We validated pressure change calculation in PSS pressure coordinate using the 3-D synthetic gas injection case (Fig. 6) that assumes high permeability reservoir surrounded by impermeable seals. The model consists of 30603 cells ($101 \times 101 \times 3$) with a single injector in the center of the reservoir, which injects gas at constant rate of 3000 MSCF/d. The reservoir is initially filled with water and is at uniform pressure (4500 psi). Black-oil type simulator (ECLIPSE E100) was used for simulation of 3-year gas injection.

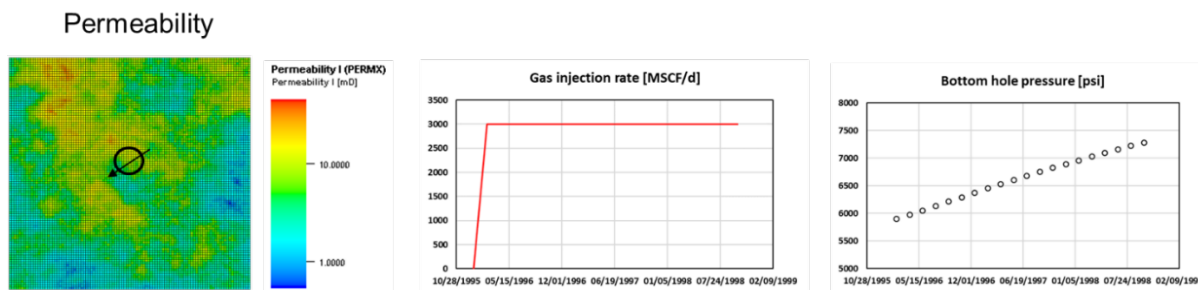


Figure 6. 3-D synthetic case: Permeability field, well rate and bottom-hole pressure

Fig. 7 shows PSS pressure and DTOF contours, multi-resolution models generated based on each pressure solution, and their simulation results compared to reference fine-scale simulation. In both multi-resolution models, 4% of total cells are preserved as fine-scale grids around the well although they differ in the geometry. The comparison of pressure change distribution after 2 years of gas injection shows close agreement between reference and PSS-SIM, and also convinces us to prefer PSS pressure to DTOF in the similar high permeability reservoirs. The BHP responses are almost identical for all three simulations for this simple example and this shows the consistency provided by the high-resolution grids retained around the well.

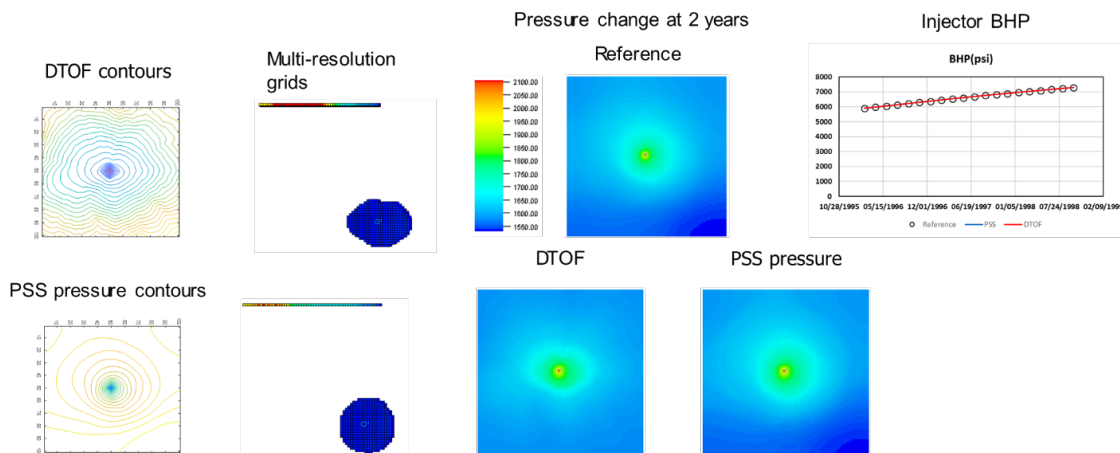


Figure 7. Pressure change comparison for simulation in DTOF-based, PSS pressure-based and fine-scale grids

Field Application

In this section, we use a simulation model of a large-scale CO₂ storage test for demonstration of the efficient pressure and mean stress change calculation in a field example and propose a quick geomechanical risk assessment using the simulation output. In the first part, we discuss the consistency and efficiency of PSS-SIM in CO₂ storage simulation through comparison of simulated pressure change and well responses with fine-scale simulation. In the second part, we show an application of the efficient simulation workflow for Fault Slip Potential (FSP) analysis (Walsh and Zoback, 2016; Lund Snee and Zoback, 2018) as induced seismicity risk assessment for the large domain of the storage site following Changqing et al. (2022).

Model Description: Illinois Basin Decatur Project (IBDP) Model

For the field-scale CO₂ storage simulation study, we use the dynamic flow model developed for the Illinois Basin-Decatur Project (IBDP). IBDP is a carbon capture and storage (CCS) project of the Midwest Geological Sequestration Consortium to inject supercritical CO₂ at a rate of approximately 1102 tons (1000 tonnes) per day for three years into the basal part of the 1640 ft (500 m) thick Mt. Simon Sandstone unit at a depth of 7025 ft (2.14 km) (Bauer et al., 2016). The IBDP model covers the large geologic domain of the CO₂ storage including reservoir, caprocks and basement, where permeability and porosity range in 1e-10 to 413md and 0 to 0.275 (**Fig. 8**). One injector (CCS1) and one monitoring well (VW1) with several pressure gauges are located roughly at center of the model. The fine-scale grids consist of 1.73 million cells (126×125×110) and we used ECLIPSE E300 (CO2STORE) with three components CO₂, H₂O and NaCl for simulation of 3 year injection and 1-year post injection under isothermal condition.

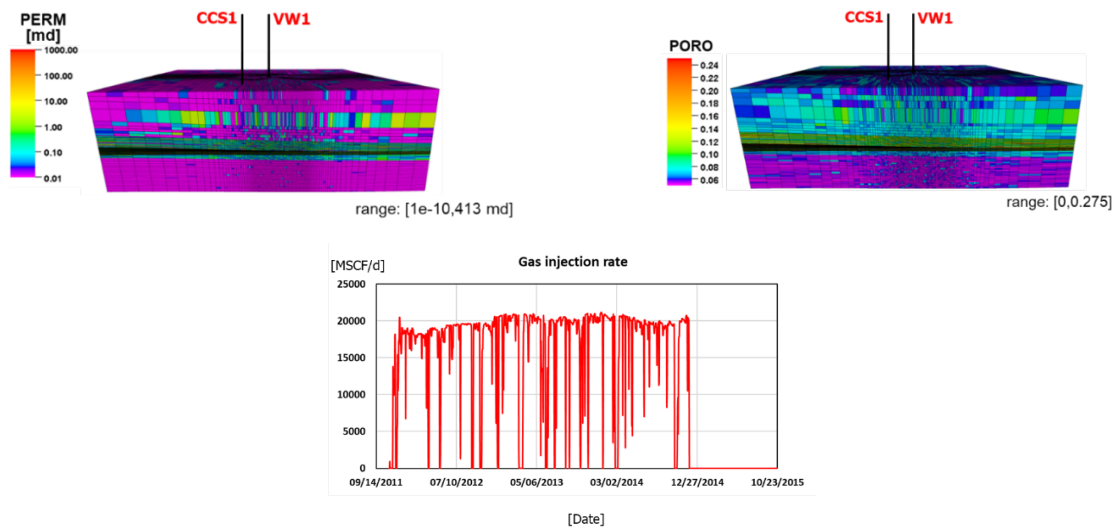


Figure 8. IBDP model description

Multi-Resolution Model

Fig. 9 shows PSS pressure contours computed for grid coarsening purpose and the resultant multi-resolution grid system. About 2% of total cells (34649) were retained as fine-scale grids, and the preserved domain covers the locations of the injector and the monitoring well. We can see that the geometry of preserved domain reflects the pressure communication in vertical direction towards the basement due to pre-existing fractures. The multi-resolution model has 4736 NNCs to define connections between outermost cells of the preserved domain and the 1st 1-D cell, and connections in the 1-D grid domain.

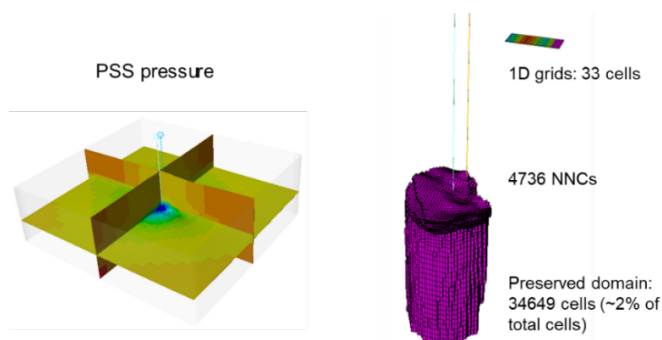


Figure 9. PSS pressure contours and preserved domain for IBDP model

Simulation Results

Fig. 10 shows comparison of well responses alongside the computational time of fine-scale and multi-resolution simulation, where WB1, WB2 and WB3 correspond to pressure gauges of the monitoring well around the injection zone. The computational time of PSS-SIM includes pre-processing time (calculation of PSS pressure, grid coarsening and reservoir property upscaling) and subsequent multi-resolution simulation time. The well responses show consistent results of PSS-SIM with the reference at both the injector and the monitoring well, while the simulation on significantly reduced grids accelerated the fine-scale simulation by ~16x on single-core simulation including the pre-processing. As shown in previous multi-resolution simulation studies, the agreement of well responses is expected to improve as more fine-scale grids are preserved at the cost of computational time.

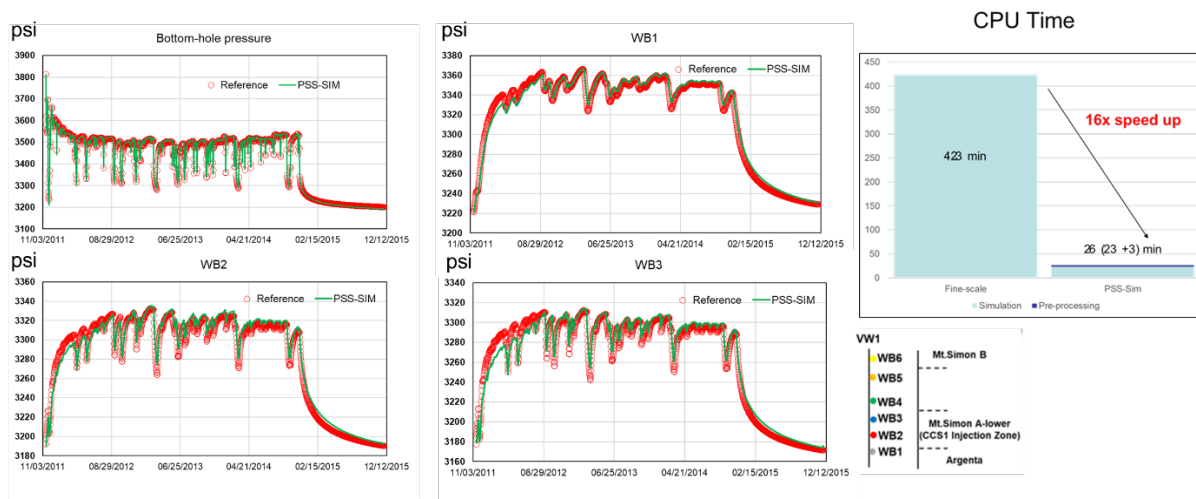


Figure 10. Comparison of well pressure (reconstructed with pressure change for PSS-SIM) and CPU time (Single core simulation)

Snapshots of pressure change are compared in **Fig. 11**, where we can visually confirm that PSS-SIM approximates reference pressure change solution well at 1, 6, 12 months from their similar contour shapes and the extent of pressure change propagation. The pressure changes of multi-resolution simulation were calculated based on averaged initial pressure and mapped back on the fine-scale grids for the comparison. The similarity in the pressure change contour shapes between two simulations become more prominent around 6 month and we can see the pressure change approaches PSS. **Fig. 12** shows mean stress change efficiently computed in the common multi-resolution grids as additional output, the use of which is demonstrated in the following geomechanical risk assessment section. The mean stress calculation will only add a few seconds of CPU time per required time step.

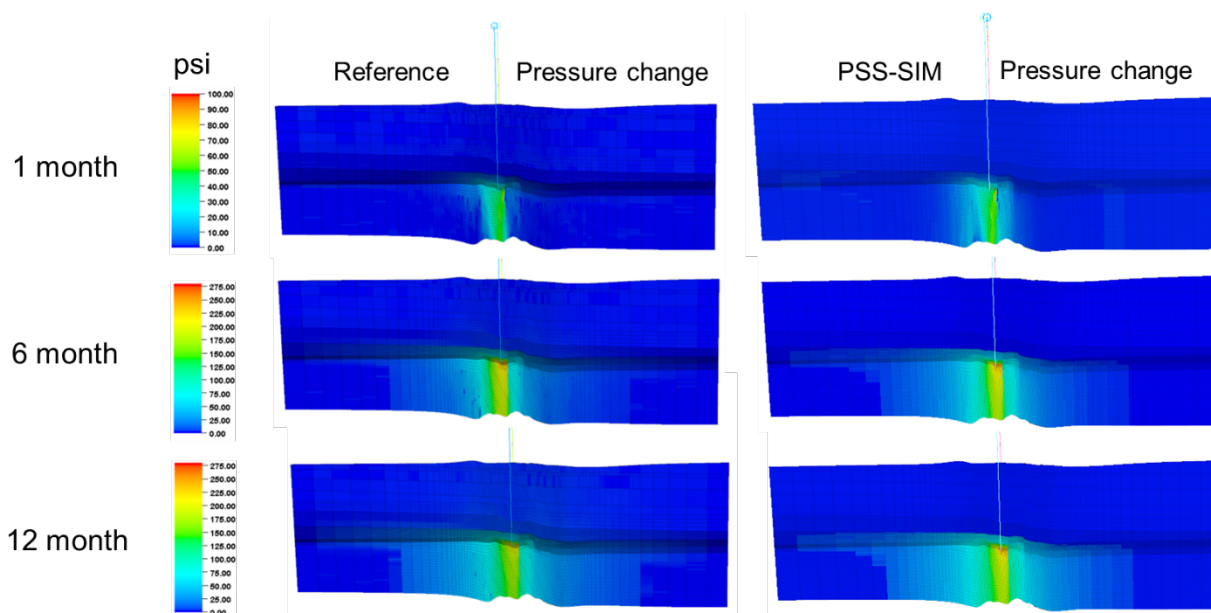


Figure 11. Pressure change comparison at 1,6,12 months

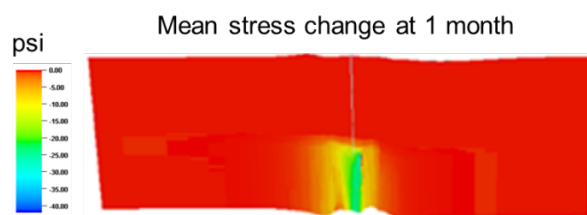


Figure 12. Mean stress change at 1 month

Fault Slip Potential (FSP) Analysis

We performed FSP analysis as a quick induced seismicity risk assessment of the CO₂ storage operation utilizing the simulated pressure and mean stress change. This analysis follows the approach in Changqing et al (2022), which investigated the induced seismicity risk of waste water injection in the Fort Worth basin based on FSP by integrating numerical simulation output. FSP determines probability of shear failure of the rock based on Mohr-Coulomb framework, where the critically stressed circumstances occur when the ratio of resolved shear stress to normal stress reaches or exceeds the failure envelop. Coulomb failure criterion is the simplest yet most widely used failure criterion which has been adopted in many fault slip risk assessment studies including Camargo et al. (2023) and Makhnenko et al. (2020). Similarly to Changqing et al (2022), our FSP calculation is Monte Carlo-type analysis where required parameters such as in-situ stress, friction coefficient etc. are randomly sampled from uniform distribution with specified parameter ranges and available simulator output is integrated to determine the probability of fault slip given the injection schedule. In this study, we demonstrate FSP calculation in two scenarios, one of which assumes the critically oriented fault exists at each location and a specific fault orientation is assumed for the other. In the first scenario, shear failure can occur when any part of the depicted Mohr's circle touches or exceeds the failure line, while the second scenario determines failure based on the shear and normal stress projected on the specified fault plane. The FSP calculated in the first case can be seen as the upper limit of FSP at the location and will be referred as "the worst scenario" in this section. It is not rare that we have little knowledge on fault locations and orientations, and similar analysis was conducted in Camargo et al. (2023). Since we have pressure and mean stress changes as simulator output, we investigate the effects of those parameters on FSP while only pressure change was utilized in

Changqing et al. (2022). We do not intend to provide any conclusion on the induced seismicity risks of the IBDP site, and it is rather a demonstration of a workflow and capability/limitation of the reduced-order simulation in the rapid geomechanical risk assessment using the IBDP model as an example. The sample parameter ranges required for the FSP calculation were selected based on Bauer et al. (2016), Camargo et al. (2023) and Makhnenko et al. (2020) (**Table 1**).

$S_{H_{max}}$ gradient(MPa/km)	$S_{H_{min}}$ gradient(MPa/km)	S_v gradient(MPa/km)	Fault μ	Cohesion
40 ± 5	21 ± 2	23.75	0.7 ± 0.05	0

Table 2. Parameter ranges for FSP calculation

First, we compare FSP increase caused by CO₂ injection in the bottom layer of the injection zone at 10 months for the worst scenario, only utilizing simulated pressure changes from fine-scale simulation and PSS-SIM (**Fig. 13**). Initial pressure of the layer is taken from the simulation model. We can see similar FSP distribution for fine-scale simulation and PSS-SIM based results, while the former takes ~ 7 hours for pressure change calculation of the entire simulation period and the latter only takes ~25 minutes, demonstrating the utility of PSS-SIM as a quick geomechanical risk assessment tool.

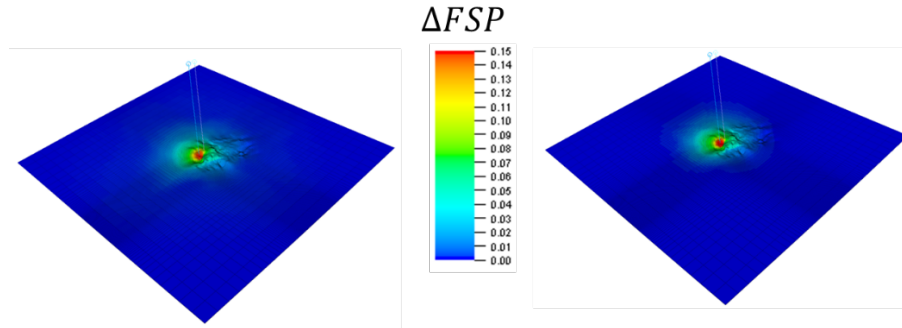


Figure 13. FSP increase estimated based on simulated pressure change from fine-scale (left) simulation vs PSS-SIM (right)

Next, we compare FSP change estimated for the same worst case scenario by using (1) pressure change only, (2) pressure and mean stress change and (3) pressure and full stress-tensor components (**Fig. 14**). Remember that PSS-SIM is capable of computing full stress-tensor components optionally with additional computational cost, which the results of (3) are based on. While the stress decomposition calculation may be afforded considering the significant CPU time savings in flow simulation, our objective here is a quick assessment using pressure and mean stress change, and (3) is only included as reference for the comparison purpose. The mean stress change was simulated with uniform Poisson's ratio of 0.2 for this study. Since mean stress change is averaged change of normal stresses in 3-D space, we make the simple assumption of uniform rock deformation at each cell, hence

$$\Delta\sigma_m = \Delta\sigma_{sh,max} = \Delta\sigma_{sh,min} = \Delta\sigma_{sv} \text{ in order to incorporate mean stress change into FSP calculation.}$$

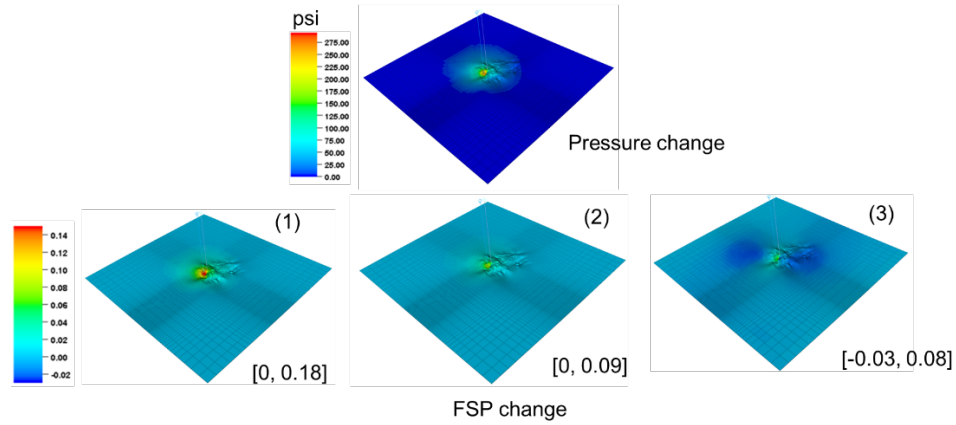


Figure 14. Pressure change and ΔFSP estimated with (1) pressure only, (2) pressure + mean stress and (3) pressure + stress tensor components

In **Fig. 14**, the range of FSP change are shown below each figure and we can see FSP increase is the highest in (1) pressure-only estimation where up to 18% increase was observed for ~ 290 psi (2 MPa) pressure buildup. With the $\Delta\sigma_m = \Delta\sigma_{sh,max} = \Delta\sigma_{sh,min} = \Delta\sigma_{sv}$ assumption, mean stress change will not cause shear stress changes on any plane as is the case for pressure change. While pore pressure increase leads to decrease of normal effective stress on fault which moves the Mohr’s circle closer to the failure line, increased compressive stress will have the opposite effects on the effective normal stress, hence lower FSP increase was estimated in (2). Compared to the reported results in Camargo et al. (2023), which similarly studied probability of shear failure on a critically oriented fault plane at the depth of injection zone for the IBDP, FSP increase in (1) seems to be overestimated even though different sample parameter distributions were used for the calculation. In fact, the effects of stress change is considered in their study through stress path factor, which is defined as ratio of horizontal stress changes to pressure change, and FSP calculated for (2) and (3) show closer values to their results. Stress path factor is given as a sample parameter in their study based on uniaxial strain assumption while our mean stress change at each cell is simulated free of such assumption, although the decomposition ratio of the mean stress for each principal stresses needs to be similarly specified.

Lastly, we estimated FSP change for two faults orientated in $200^\circ, 300^\circ \pm 7.5$ from the north with dip angles of $70^\circ \pm 5$ assuming the direction of maximum horizontal stress is in $N68^\circ E \pm 4$. For simplicity, x-axis of the simulation model is assumed to be aligned with the north. The results are shown in **Fig. 15**, where the top row corresponds to fault orientated in 200° and the bottom row is for 300° case.

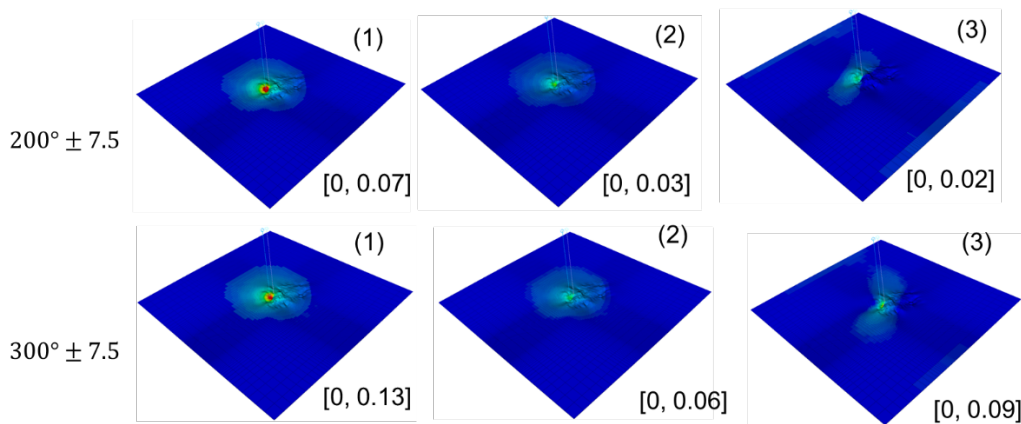


Figure 15. ΔFSP estimated at two fault planes based on (1) pressure only, (2) pressure + mean stress, (3) pressure + stress tensor components

FSP increases calculated for specific fault planes mostly fall below the ones estimated for the worst scenario. Similarly to the results in the worst scenario, pressure-only approach seems to overestimate FSP increase compared to the reference solution, indicating a certain advantage of having mean stress change as additional information although it carries limited information compared to full stress-tensor components. FSP calculated with full stress-tensor components differ from the other solutions because of the different ratio of horizontal stress changes than the one assumed for mean stress based estimation, and also because of the effects of shear stress changes not accounted in the other solutions. The difference in spatial distribution clearly reflects those effects, and they are compromised in other solutions for the simulation efficiency. To summarize this study, we have demonstrated the capability of PSS-SIM to assess pressure-induced geomechanical risks of the CO₂ injection within a realistic timeframe, and the simplistic geomechanics simulation to provide mean stress change with minimal computational cost increase showed a certain value in the risk assessment, where conventional geomechanics simulation is usually not feasible in field-scale problems.

Conclusions

We have developed multi-resolution coupled flow and geomechanics simulation tool that uses PSS pressure solution as spatial coordinate (PSS-SIM) for efficient dynamic modeling of CO₂ storage as a part of the Science-informed Machine Learning (ML) for Accelerating Real-Time Decisions in Subsurface Applications (SMART) Initiative. In the PSS-SIM workflow, 1-D grid coarsening along PSS pressure solution significantly reduces grid dimension of the model for faster computation while consistency is preserved by high resolution grids retained around wells. The use of PSS pressure contours as spatial coordinate is based on the knowledge of flow patterns in the typical CCS reservoirs, and it can be computed with initial reservoir properties with reasonable CPU time as a part of pre-processing. PSS-SIM is capable of efficient mean stress change calculation in addition to pressure change by taking advantage of MS-based equation that is compatible with the PSS pressure-based grids, where computational time of typical coupled simulator is expected to be prohibitive in large-scale CCS applications. The accuracy of PSS-SIM was verified with the 3-D synthetic case against fine-scale simulation, and also showed consistent results in the field example with more than an order-of-magnitude speed up. The FSP analysis demonstrated as a part of the field application showed the utility of PSS-SIM as a quick geomechanical risk assessment tool while the inevitable modeling error needs to be understood as the price for the significant speed up. Extension of the coupled simulation workflow to the two-way coupling scheme to account for the geomechanical effects on flow remains a future project as this workflow can benefit more from efficiently computed mean stress change in the two-way coupling.

References

- Bauer, Robert A., Carney, Michael, Finley, Robert J., Overview of microseismic response to CO₂ injection into the Mt. Simon saline reservoir at the Illinois Basin-Decatur Project, *International Journal of Greenhouse Gas Control*, Volume 54, Part 1, 2016, Pages 378-388, ISSN 1750-5836, <https://doi.org/10.1016/j.ijggc.2015.12.015>.
- Chen, Hongquan, Onishi, Tsubasa, Park, Jaeyoung, and Akhil Datta-Gupta. "Computing Pressure Front Propagation Using the Diffusive-Time-of-Flight in Structured and Unstructured Grid Systems via the Fast-Marching Method." *SPE J.* 26 (2021): 1366–1386. <https://doi.org/10.2118/201771-PA>.
- Chen, Hongquan, Terada, Kazuyuki, Li, Ao, and Akhil Datta-Gupta, 2022. Rapid Simulation of Unconventional Reservoirs Using Multi-Domain Multi-Resolution Discretization Based on the Diffusive Time of Flight. Paper presented at the SPE/AAPG/SEG Unconventional Resources Technology Conference, Houston, Texas, USA, June. doi: <https://doi.org/10.15530/urtec-2022-3723026>.

Fujita, Y., Datta-Gupta, A. & M.J.King, 2016. A Comprehensive Reservoir Simulator for Unconventional Reservoirs That Is Based on the Fast-Marching Method and Diffusive Time of Flight. *SPE Journal*, 21(6), pp. 1-13. <https://doi.org/10.2118/173269-PA>.

Hu, L., Winterfeld, P. H., Fakcharoenphol, P. & Wu, Y.-S., 2013. A novel fully-coupled flow and geomechanics model in enhanced geothermal reservoirs. *Journal of Petroleum Science and Engineering*, Volume 107, pp. 1-11. doi: <https://doi.org/10.1016/j.petrol.2013.04.005>.

Iino, Atsushi , Vyas, Aditya , Huang, Jixiang , Datta-Gupta, Akhil , Fujita, Yusuke , Bansal, Neha , and Sathish Sankaran, 2017. Efficient Modeling and History Matching of Shale Oil Reservoirs Using the Fast Marching Method: Field Application and Validation. Paper presented at the SPE Western Regional Meeting, Bakersfield, California, April. doi: <https://doi.org/10.2118/185719-MS>.

IPCC. (2005). Carbon Dioxide Capture and Storage. <https://www.ipcc.ch/report/carbon-dioxide-capture-and-storage/>

Lund Snee, J.-E., & Zoback, M. D. (2018). State of stress in the Permian Basin, Texas and New Mexico: Implications for induced seismicity. *The Leading Edge*, 37, 127–134. <https://doi.org/10.1190/tle37020127.1>.

Nagao, Masahiro, Yao, Changqing, Onishi, Tsubasa, Chen, Hongquan, and Akhil Datta-Gupta. "An Efficient Deep Learning-Based Workflow for CO2 Plume Imaging With Distributed Pressure and Temperature Measurements." *SPE J.* 28 (2023): 3224–3238. doi: <https://doi.org/10.2118/210309-PA>.

Nakajima, Kenta and Michael King. "Development and Application of Fast Simulation Based on the PSS Pressure as a Spatial Coordinate." Paper presented at the SPE Annual Technical Conference and Exhibition, Dubai, UAE, September 2021. doi: <https://doi.org/10.2118/206085-MS>.

Onishi, Tsubasa, Iino, Atsushi, Jung, Hye Young, and Akhil Datta-Gupta. "Fast Marching Method Based Rapid Simulation Accounting for Gravity." Paper presented at the SPE/AAPG/SEG Asia Pacific Unconventional Resources Technology Conference, Brisbane, Australia, November 2019. <https://doi.org/10.15530/AP-URTEC-2019-198249>.

Pruess, K., García, J. Multiphase flow dynamics during CO2 disposal into saline aquifers. *Env Geol* 42, 282–295 (2002). <https://doi.org/10.1007/s00254-001-0498-3>.

Sethian, J. A. 1999. Fast Marching Methods. *SIAM Rev*41 (2): 199–235. <https://doi.org/10.1137/S0036144598347059>.

Terada, Kazuyuki "Rapid Coupled Flow and Geomechanics Simulation using the Fast Marching Method." Paper presented at the SPE Annual Technical Conference and Exhibition, Calgary, Alberta, Canada, September 2019. <https://doi.org/10.2118/199785-STU>.

Terada, Kazuyuki, Chen, Hongquan, Iino, Atsushi, and Akhil Datta-Gupta. "Multi-Resolution Coupled Flow and Geomechanics Modeling Using Fast Marching Method." Paper presented at the SPE/AAPG/SEG Unconventional Resources Technology Conference, Denver, Colorado, USA, June 2023. doi: <https://doi.org/10.15530/urtec-2023-3859799>.

Wang, Shihao, Wu, Yu-Shu, Theoretical analysis and semi-analytical formulation for capturing the coupled thermal-hydraulic-mechanical process using the stress formulation, *Journal of Petroleum Science and Engineering*, Volume 208, Part D, 2022, 109752, ISSN 0920-4105, <https://doi.org/10.1016/j.petrol.2021.109752>.

Yao, Changqing, Park, Jaeyoung, Chen, Hongquan, Datta-Gupta, Akhil, Hennings, Peter, and Robin Domisse. "High Resolution Modeling of Pore Pressure Change, Fault Slip Potential and Induced Seismicity in the Fort Worth Basin." Paper presented at the SPE Western Regional Meeting, Anchorage, Alaska, USA, May 2023. doi: <https://doi.org/10.2118/212951-MS>.

Zhang, Y., N.Bansal & Y.Fujita, 2016. From Streamlines to Fast Marching: Rapid Simulation and Performance Assessment of Shale-Gas Reservoirs by Use of Diffusive Time of Flight as a Spatial Coordinate. SPE Journal, 21(5), 1-16. <https://doi.org/10.2118/168997-PA>.

Zheng, Fangning , Jahandideh, Atefeh , Jha, Birendra , and Behnam Jafarpour. "Quantification and Incorporation of Geomechanical Risks in Optimization of Geologic CO2 Storage Using Coupled-Physics Models." Paper presented at the SPE Annual Technical Conference and Exhibition, Virtual, October 2020. doi: <https://doi.org/10.2118/201499-MS>.

Zhou, Quanlin, Birkholzer, Jens T., Tsang, Chin-Fu, Rutqvist, Jonny. "A method for quick assessment of CO2 storage capacity in closed and semi-closed saline formations." International Journal of Greenhouse Gas Control, Volume 2, Issue 4, 2008, Pages 626-639, ISSN 1750-5836, <https://doi.org/10.1016/j.ijggc.2008.02.004>.

Walsh, F. Rall, Zoback, Mark D; Probabilistic assessment of potential fault slip related to injection-induced earthquakes: Application to north-central Oklahoma, USA. Geology 2016;; 44 (12): 991–994. doi: <https://doi.org/10.1130/G38275.1>.

Winterfeld, P. H., and Wu, Yu-Shu. Simulation of Coupled Thermal-Hydrological-Mechanical Phenomena in Porous and Fractured Media, 2015. Paper presented at the SPE Reservoir Simulation Symposium, Houston, Texas, USA, February. doi: <https://doi.org/SPE-173210-MS>.

Winterfeld, P. H., and Wu, Yu-Shu. "Coupled Reservoir-Geomechanical Simulation of Caprock Failure and Fault Reactivation During CO2 Sequestration in Deep Saline Aquifers." Paper presented at the SPE Reservoir Simulation Conference, Montgomery, Texas, USA, February 2017. doi: <https://doi.org/10.2118/182605-MS>.